Magnetite Particle Size Distribution and Pellet Oxidation

HYEON JEONG CHO, MING TANG, and PETRUS CHRISTIAAN PISTORIUS

Oxidation of magnetite pellets is commonly performed to prepare strong pellets for ironmaking. This article presents a contribution to quantitative understanding of fundamental pellet oxidation kinetics, based on measured oxidation kinetics of magnetite particles and pellets. The commonly observed ''plateau'' oxidation behavior is confirmed to be consistent with the effect of very large differences in magnetite particle sizes in the concentrate from which pellets are produced. The magnetite particles range in size from less than a micron to several tens of a microns; changing the size distribution by inert sintering of pellets decreases both the plateau level of oxidation and the specific surface area, in ways that are compatible with an assumed Rosin-Rammler magnetite particle size distribution.

DOI: 10.1007/s11663-014-0104-1

I. BACKGROUND

MAGNETITE concentrates are widely used to produce hematite pellets for ironmaking. During firing, green pellets (magnetite concentrate with bentonite binder, rolled into approximately spherical pellets) are heated and exposed to oxygen-containing gas (using a grate-kiln process in many cases). Firing oxidizes magnetite to hematite. Pellet strength relies on the physical bonds formed between oxidized particles; fine outgrowths form on the oxidized particle surfaces,[1] favoring formation of bonds between particles.

One possible cause of poor pellet strength (after firing) is the incomplete oxidation of pellet cores. Prediction of the size of unoxidized cores would require accurate information on magnetite oxidation kinetics. The oxidation of magnetite pellets at temperatures up to approximately 1200 K (or approximately 900 °C), in air or atmospheres containing similar oxygen concentrations, is controlled or partially controlled by solid-state diffusion through a hematite product layer that forms in the magnetite particles during oxidation.[2–4]

Prediction of the oxidation of magnetite pellets under mixed control, where gaseous diffusion of oxygen into pellets can be partially rate-limiting, is the topic of a companion paper.[5] This article focuses on the oxidation kinetics of concentrate particles in the absence of gas mass transfer limitations, and the effect of particle size distribution on overall oxidation kinetics. Particle size effects in oxidation of magnetite pellets were previously studied by Forsmo *et al.*,[6] who found that finer concentrates did oxidize faster (during continuous heating in 16 pct O_2). However, gaseous oxygen mass transfer undoubtedly limited the observed oxidation rate in the work of Forsmo *et al.*,[6] as shown by a dependence of oxidation extent on oxygen pressure. The work presented in this article specifically aimed to eliminate gaseous oxygen transfer as a rate-limiting step when considering particle size effects.

To a first approximation, the effect of particle size on oxidation rate (in the absence of limitation by gaseous oxygen mass transfer) can be described by parabolic kinetics.[7] If each particle were approximately spherical, and hematite would form a continuous product layer within each oxidizing particle, then oxidation would be described by simple shrinking-core kinetics, as follows:

$$t = \left[d^2/(24k_p)\right] \times \left[3 - 2f - 3(1-f)^{2/3}\right] \qquad [1]$$

where t is the oxidation time, d is the magnetite particle diameter, k_p is the parabolic rate constant, and f is the degree of oxidation. The results presented later in this article show that magnetite particles from plant concentrate do follow this relationship approximately. Oxidation of individual magnetite particles does not follow this relationship exactly, for several reasons: First, concentrate particles are not spherical. Second, hematite often does not grow along a uniform front advancing into the magnetite pellets, but rather as laths or lamellae.[8] Lamellar or lathlike growth of hematite into magnetite occurs because densely packed (1000) planes of hematite align parallel with densely packed (111) planes of magnetite[9]; the same orientation relationship is observed during reduction of hematite to magnetite.[10] Despite the partially lathlike reaction front, simple shrinking-core kinetics based on assumed spherical particles were found to approximate oxidation of magnetite concentrate particles (screened to 74 to 100 μm),[7] and this approach was also followed in this work. The results presented later in this article indicate that departure from simple shrinking-core kinetics results in the apparent parabolic rate constant decreasing by a factor of approximately two, from faster initial oxidation to full oxidation. This change

HYEON JEONG CHO, formerly a Graduate Student with the Department of Materials Science and Engineering, Carnegie Mellon University, Pittsburgh, PA, is now Assistant Manager with the Technical Research Center, Hyundai Steel, Dangjin, South Korea. MING TANG, Research Assistant, and PETRUS CHRISTIAAN PISTORIUS, Professor, are with the Department of Materials Science and Engineering, Carnegie Mellon University. Contact e-mail: pistorius@cmu.edu

Manuscript submitted December 13, 2013.
Article published online July 9, 2014.

is much smaller than the effect of particle size; as shown later in this article, the largest particles in typical concentrate particles are approximately a thousand times larger in diameter than the smallest particles, resulting in a difference in rate of oxidation of six orders of magnitude (because oxidation approximately follows parabolic kinetics as described by Eq. [1]).

This article tests the suggestion that the very strong effect of concentrate particle size on oxidation rate, and the wide size range of concentrate particles, together cause the unusual oxidation behavior of pellets prepared from magnetite concetrate.[1] As documented early in the development of the taconite pellet process,[4] oxidation of magnetite pellets does not follow simple shrinking-core kinetics. Isothermal oxidation of pellets reaches a plateau level; the plateau depends on temperature and on concentrate source, and an example is given Figure 1. During isothermal oxidation, the smallest particles would oxidize very rapidly (approximately following parabolic kinetics), whereas the largest particles would remain largely unoxidized; the plateau level hence simply reflects the proportion of particles that oxidized at the particular temperature.

In the work presented in this article, the suggestion was tested that the magnetite particle size distribution controls plateau oxidation behavior. The test involved changing the size distribution of magnetite particles in pellets by sintering pellets under inert conditions and subsequently measuring the specific surface area of the pellets (as an indication of average magnetite particle size), as well as the oxidation behavior. If the particle size distribution were to control the plateau behavior as suggested, then sintering (which would eliminate smaller particles) would lead to a lower oxidation plateau.

As before, the concentrate was approximated as a collection of spherical particles that follows a Rosin-Rammler size distribution as shown in Eq. [2][11]:

$$R = \exp[-(d/d*)^n] \qquad [2]$$

where R is the mass fraction of particles that have a diameter larger than d. The parameters of the distribution are d^* and n. The parameter d^* is a type of average diameter because $1/e = 36.8$ pct (by mass) of the particles are larger than d^*, and $1 - 1/e = 63.2$ pct of particles are smaller than d^*. The parameter n describes the width of the size distribution around d^*: Smaller values of n give wider size distributions; reasonable values of n appear to be between 0.5 and 2.5.[12]

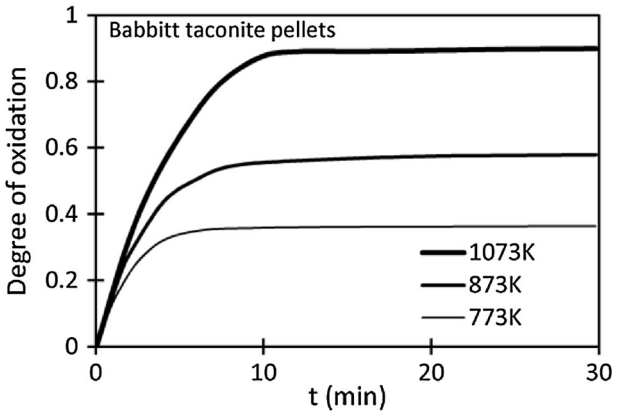

Fig. 1—Oxidation of Babbitt taconite pellets in air, at three different temperatures. Redrawn from the results of Zetterstrom.[4]

II. EXPERIMENTAL APPROACH

A. *Raw Materials*

Magnetite concentrate and green (unfired) pellets (bentonite binder approximately 0.5 pct of pellet mass) were received from an operating mine in the Mesabi range. The chemical compositions of the concentrate and pellets are summarized in Table I.

The as-received concentrate had a very large range of particle sizes (see Figure 2). The particle size distribution is so wide that no single microscopic technique was successful in quantifying the size range; attempts to quantify the size range were also hampered by clustering of the magnetic particles. However, it is quite clear the particle size range is large. Optical microscopy and scanning electron microscopy both showed the largest particles to be tens of microns in diameter (see Figure 2 for examples). Transmission electron microscopy (TEM) was used to estimate the smallest particle sizes. Although the limited number and size range of concentrate particles that can be examined by TEM do not allow quantification of the size range, particles as small as 10 nm were found by TEM of concentrate samples. Based on these observations, the ratio of the largest to the smallest particle diameters is at least 1000. The specific surface area of pellets was measured by BET adsorption (nitrogen pressure range 0.01 to 0.025 atm), to give an estimate of average particle size. Attempts to use light scattering and a Coulter tube method to measure the size distribution of concentrates were unsuccessful because of their wide size range (resulting in settling of larger particles while the smaller particles remain in suspension), as well as the tendency of the magnetite particles to clump together magnetically (increasing the apparent particle size).

To study size effects and the inherent oxidation behavior separately, a narrow size fraction (53 μm to 63 μm) of the concentrate was prepared by wet screening (see Figure 2).

B. *Oxidation Rate Measurements*

Thermogravimetric analysis (TGA) was used to determine isothermal oxidation rates. For measurement of the parabolic rate constant for oxidation, magnetite particles in the 53 to 63 μm size fraction were tested. The particles (1 g per test) were contained in an alumina crucible (inner diameter 11 mm and the height 22.5 mm) and hung at the center of a vertical quartz tube furnace. The typical sample depth in the crucible was around 14 mm. The sample was first heated in nitrogen from room temperature to the test temperature of 773 K, 873 K or 1073 K (500 °C, 600 °C, or 800 °C) at a heating rate of 20 K/min, and then the gas atmosphere

was switched to a mixture of oxygen and nitrogen, measuring mass gain for periods of up to 24 hours. For the oxygen contents used here (20 pct and higher), the oxidation rate was found not to depend on the oxygen contents of the gas, apart from a small dependence during an initial period of approximately 4 minutes (immediately after switching the input gas from pure nitrogen to the nitrogen-oxygen mixture). The procedure was similar for pellets; single pellets were oxidized, using a wire cage to hang the pellets at the center of the furnace. All pellets were oxidized for 30 minutes at 600 °C (873 K, using a gas mixture of 80 pct N_2-20 pct O_2). The pellets were approximately spherical, with diameters around 1 cm. At this temperature and oxygen content, the pellets oxidized uniformly, with no macroscopic reaction front.

During heating and oxidation, the temperature in the hot zone of the furnace was monitored with a K-type thermocouple. The tip of the thermocouple was approximately 10 mm below the sample (pellet, or crucible with particles), within the furnace tube. A small temperature increase was observed at the start of oxidation, after switching from nitrogen to oxygen-containing gas. The extent of the temperature increase was approximately 10 K at a setpoint of 873 K (600 °C), and approximately 5 K at 1073 K (800 °C). The small temperature increase disappeared after some time, typically 30 minutes at 873 K (600 °C) and 50 minutes at 1073 K (800 °C).The cause of the temperature increase is the exothermicity of magnetite oxidation. Given the small extent of the temperature increase and the small apparent activation energy of magnetite oxidation (as shown in the results presented in this article), these temporary temperature excursions did not affect oxidation kinetics significantly, for the temperatures considered here. This is similar to the conclusion reached by Papanastassiou and Bitsianes.[9]

Table I. Chemical Compositions of Raw Materials (Mass Percentages)

	Concentrate	Pellets
Fe	67.86	65.20
SiO_2	4.44	4.79
Al_2O_3	0.25	0.41
CaO	0.49	0.84
MgO	0.540	0.560
Mn	0.220	0.220
P	0.021	0.021
Na_2O	0.033	0.046
K_2O	0.014	0.022

After oxidation, phase fractions were measured by X-ray diffraction (XRD), using Cu-Kα radiation, step of 0.05 deg, and 2 seconds/step, with 10 deg to 80 deg 2Θ. The pellets were pulverized using a tungsten carbide puck mill before diffraction measurements. The weight percentages of phases were quantified from the X-ray data by the Rietveld method and by means of the relative heights of magnetite and hematite peaks (giving the same results). The relative amounts of the phases were used to quantify the degree of oxidation from the TGA mass gain data (using the XRD results to correct for the presence of gangue that did not contribute to mass gain, and in pellets bentonite binder that lost mass during oxidation). The use of Cu-Kα radiation with Fe-rich samples leads to an increase in background radiation due to secondary fluorescence.[13] To test whether this affected phase quantification, samples were prepared with several different known ratios of hematite (fully oxidized concentrate) to magnetite (unoxidized concentrate); it was found that X-ray diffraction and Rietveld quantification yielded the phase ratios accurately.

Optical microscopy (using polarized light) was used to examine polished cross-sections of oxidized pellets; with suitable alignment of polarization, hematite appears bright and magnetite darker.

To assess the effect of magnetite particle size on oxidation, the pellets first were sintered under inert conditions (high-purity nitrogen or high-purity argon) for 30 minutes, at temperatures from 1073 K (800 °C) to

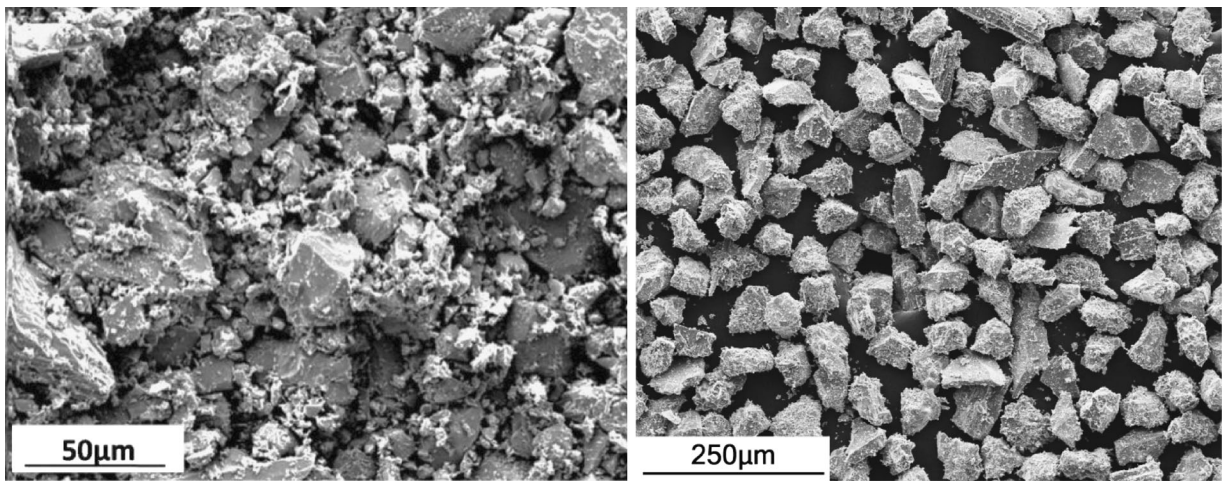

Fig. 2—Scanning electron micrographs (secondary electron images) of Mesabi-range taconite concentrate, as received (left) and after wet screening to isolate the 53 to 63 μm size range (right). (Magnifications differ.).

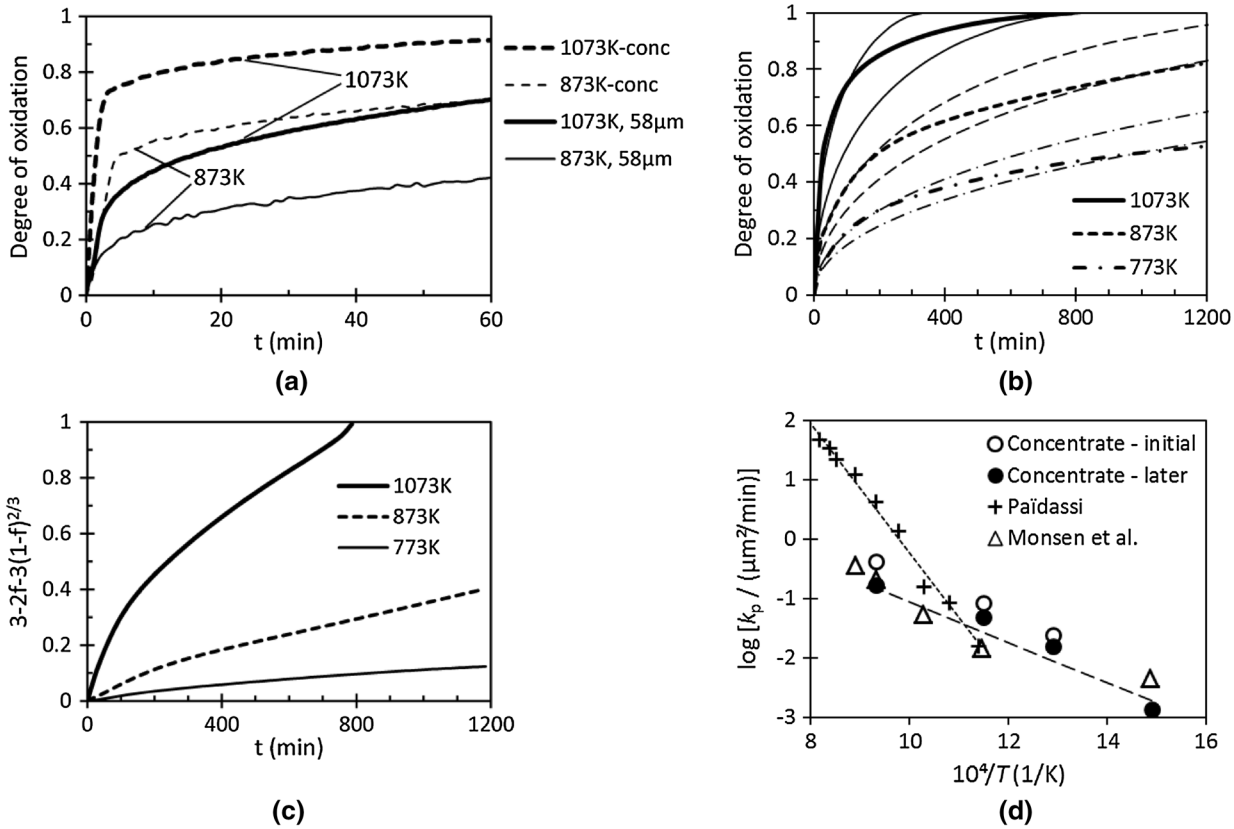

Fig. 3—Oxidation kinetics. (*a*) Oxidation of the full size range of concentrate (curves labeled "conc"), and narrow 53 to 63 μm size fraction (curves labeled 58 μm), at 873 K and 1073 K. (*b*) Longer-term oxidation kinetics of 53 to 63 μm size fraction; (*c*) the same data, plotted as $[3 - 2f - 3(1 - f)^{2/3}]$ *vs* time. (*d*) Comparison of fitted parabolic rate constants for concentrate oxidation (circles and triangles), with oxidation of magnetite in iron oxide films (crosses). (Data used in (b) and (c) reproduced with permission of the Association for Iron and Steel Technology[14]). In (b), heavier lines are experimental data; fitted kinetic curves (assuming simple shrinking-core kinetics of spherical particles) are shown as the thinner lines (two curves for each temperature, for initial and later apparent parabolic rate constants).

1373 K (1100 °C) (heating and cooling rate to holding temperature 5 K/min). These temperatures are above the sintering temperature for magnetite, and hence agglomeration of fine magnetite was expected to occur. The extent of sintering was assessed by measuring specific surface area. No significant change in pellet size was observed after sintering. The sintered pellets were subsequently oxidized isothermally at 873 K (600 °C) (heating to this temperature at 20 K/min in pure nitrogen, then switching to a N_2-20 pct O_2 mixture for 30 minutes when the temperature reached 873 K [600 °C], and cooling under pure nitrogen after oxidation). Because pellets were crushed into millimeter-sized pieces for BET measurements, different pellets (prepared under the same conditions) were used for BET and oxidation measurements. Based on repeat tests, the variability of the oxidation results is less than ±1 pct between tests, and that of the specific surface area less than 0.02 m^2/g.

III. RESULTS AND DISCUSSION

A. *Oxidation Kinetics*

The measured oxidation behavior of magnetite concentrates (wide size range), and of 53- to 63-μm particles (narrow size range) is summarized in Figure 3. (The oxidation behavior of the 53- to 63-μm particles was first presented in an earlier paper.[14]) The difference between oxidation of the narrowly sized (approximately 58 μm diameter) particles and the full concentrate is evident: Early oxidation of the concentrate is much faster; this result gives qualitative support to the suggested effect of the particle size distribution on the "plateau" behavior. (In Figure 3, the measured oxidation behavior of the concentrate does not show a completely level plateau; however, the concentrate did oxidize much faster initially, and much slower later, than expected for narrowly sized magnetite particles individually following shrinking-core kinetics.)

To allow a more quantitative test, the parabolic rate constant was estimated from the slope of the graph obtained by plotting the oxidation data (of the 53 to 63 μm particles) according to Eq. [1] (see Figures 3(b) and (c)). If oxidation exactly followed Eq. [1], then the plot in Figure 3(c) would be a straight line. Actual oxidation behavior is faster than expected initially (a higher slope is observed for early oxidation), in line with previous work.[7] As mentioned, likely causes of this behavior are nonspherical particle shapes (see Figure 2; sharp asperities would oxidize faster) and some lath-shaped growth of hematite into magnetite (instead of a product layer of

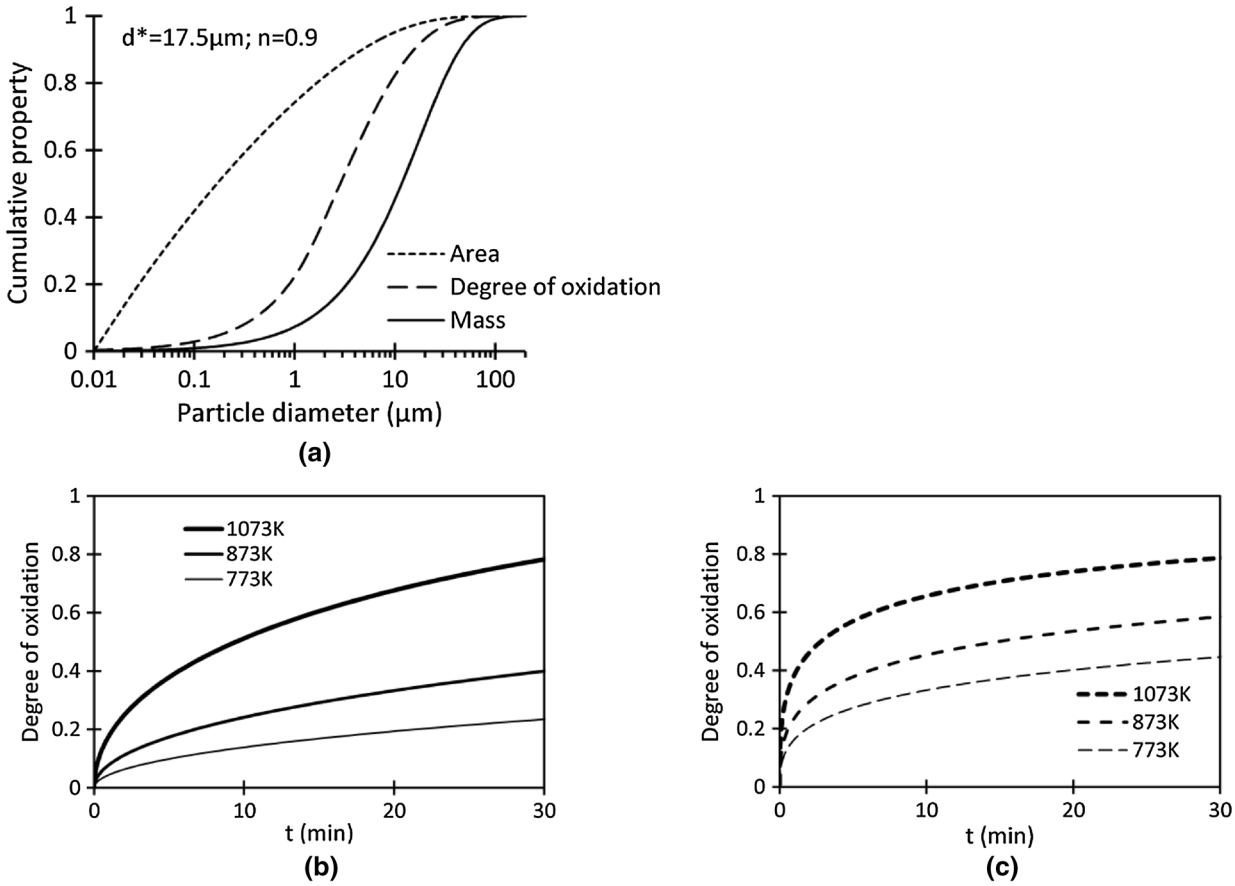

Fig. 4—Examples of calculated concentrate properties. (*a*) Cumulative area, degree of oxidation (after 30 min at 873 K [600 °C]) and mass, for magnetite concentrate following a Rosin-Rammler size distribution with $d^* = 17.5$ μm, $n = 0.9$, and minimum particle size of 0.01 μm. (*b*) Oxidation of spherical particles with a diameter of 17.5 μm, at different temperatures. (*c*) Oxidation of magnetite concentrate following a Rosin-Rammler size distribution ($d^* = 17.5$ μm; $n = 0.9$) at different temperatures.

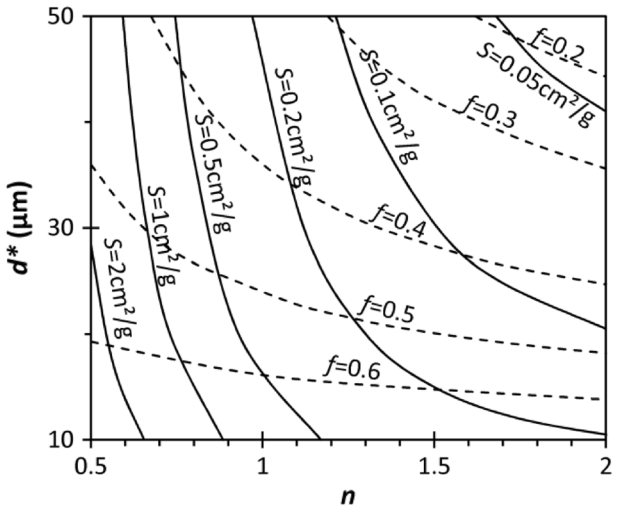

Fig. 5—Calculated specific surface area (*S*, solid lines) and degree of oxidation (*f*, broken lines) after 30 min at 873 K, for magnetite concentrates following Rosin-Rammler size distributions with different values of d^* and n, with a minimum particle size of 0.01 μm.

even thickness; see the micrographs presented in Figure 7). Despite these deviations, Eq. [1] seems to give a reasonable description of actual particle oxidation and was used in subsequent predictions of the oxidation behavior of magnetite concentrates (containing a wide range of particle sizes).

In Figure 3(d), the fitted parabolic rate constants are compared with those derived from the oxidation behavior reported by Païdassi,[15] and rate constants fitted to the results of Monsen *et al.*[7] In Païdassi's work, planar films of wüstite were oxidized, resulting in simultaneous growth of magnetite and hematite. The parabolic rate constant for oxidation of magnetite to hematite was estimated from the reported changes in hematite thickness by using the relationships of Yurek *et al.*[16] Monsen *et al.*[7] measured oxidation of suspended concentrate particles, with the size range 74 to 100 μm. A comparison of the rate constants for oxidation of magnetite films and magnetite concentrate particles (Figure 3(d)) shows a lower apparent activation energy for the latter, probably reflecting the effect of lath-like hematite growth (rather than planar growth, as observed by Païdassi). The rate constants found in this work can be seen to be similar to those calculated from the results of Monsen *et al.*[7]

In Figure 3(d), two sets of fitted parabolic rate constants are shown for this work: for each temperature, one apparent rate constant was found from the initial rate of oxidation, and another from the extent of

Table II. Measured Specific Surface Area (*S*) of Magnetite Pellets After Inert Sintering at Different Temperatures*

T_{sinter}, K	*S*, m^2/g	*F*, (-)	*d**, μm	*n*, (-)
None	1.123	0.59	17.5	0.73
1073	0.605	0.59	17.5	0.91
1223	0.254	0.56	17.5	1.3
1273	0.207	0.55	17.5	1.4
1373	0.063	0.48	17.5	4

*In this table, the measured degree of oxidation (*f*) during subsequent oxidation in 80 pct N_2-20 pct O_2 at 873 K (600 °C), and the Rosin-Rammler parameters (*d** and *n*) fitted to the specific surface area and oxidation behavior.

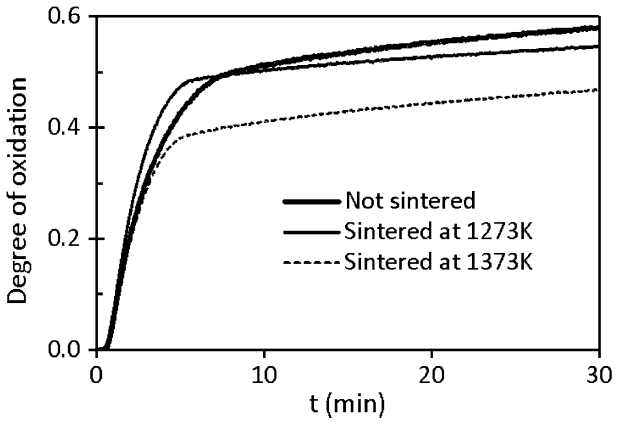

Fig. 6—Oxidation behavior at 873 K (600 °C), of pellets previously sintered in argon at different temperatures.

oxidation at the end of the oxidation period of 20 to 24 hours. Figures 3(c) and (d) show that the initial and later apparent rate constants differed by a factor of approximately two. The slower oxidation at longer times probably reflects the changing nature of the oxidation front, from initially lamellar, to a more continuous hematite layer at higher degrees of oxidation.[7,8] However, it should be noted that the slowdown in oxidation of narrowly sized (large) concentrate particles at higher degrees of oxidation is much less marked than that of concentrate with a wide size range: The examples in Figure 3(a) (for two temperatures) illustrate the difference in oxidation behavior of the full size range of concentrate (“conc” in the figure labels) and for narrowly sized concentrate particles (“58 μm” in the figure labels). The full size range of concentrate shows an abrupt decrease in oxidation rate after approximately 5 minutes, whereas the 58-μm particles show smooth increases in the extent of oxidation with increased time, approximately following simple shrinking-core kinetics.

B. *Predicted Oxidation Behavior of Magnetite Concentrate with Wide Size Distribution*

The parameters (*d** and *n*) of the Rosin-Rammler size distribution were fitted by matching the observed oxidation behavior and specific surface area of pellets (with and without prior inert sintering). For oxidation at 873 K (600 °C) for 30 minutes as considered in this article, the fitted parabolic rate constant (0.028 μm^2/min) indicates that all particles smaller than approximately 4.5 μm in diameter would be fully oxidized, whereas large particles would be expected to have a hematite product layer thickness of $(2k_p t)^{0.5} = 1.3$ μm around a magnetite core (for particles with diameters much larger than the product layer thickness, and hence an approximately planar oxidation front).

To calculate the overall degree of oxidation of concentrate that follows the Rosin-Rammler distribution, the particle size range was divided into 100 subintervals, using a geometric sequence, considering particles in the size range 0.01 μm to 200 μm, and assuming that each subset of particles follows Eq. [1]. The same size range was used to calculate the specific surface area, but using 1000 intervals, and assuming each particle to be dense magnetite with a density of 5.17 g/cm^3. It was found that the degree of oxidation was not very sensitive to the lower bound of the size range, but the specific surface area was quite sensitive to the lower bound. The lower bound of 0.01 μm was selected based on transmission electron microscopy, as mentioned earlier.

Figure 4 gives examples of calculated oxidation behavior and specific surface area for concentrate with a wide size distribution (Figures 4(a) and (c)) and theoretical monodisperse magnetite particles (Figure 4(b)). Figure 4(c) shows plateau-like behavior similar to actual concentrate and shows that the predicted degree of oxidation after 30 minutes is a weaker function of temperature than for monodisperse particles—again in line with the observed behavior, examples of which are shown in Figures 1 and 3(a).

Figure 4(a) shows the calculated contributions of the different size fractions to the total mass (Rosin-Rammler distribution), the total area, and the total degree of oxidation after 30 minutes at 873 K (600 °C). Evidently, the particles smaller than 1 μm contribute most of the area, whereas particles between 1 and 10 μm contribute most of the measured degree of oxidation. Because the specific surface area and the overall degree of oxidation are sensitive to different size fractions of the concentrate, these concentrate properties differ in their sensitivity to the parameters of the Rosin-Rammler size distribution. Figure 5 illustrates this in more detail—showing that the degree of oxidation is primarily sensitive to the average size (*d**), whereas the specific surface area is more sensitive to the width of the size distribution (expressed by *n*).

C. *Sintered pellets*

For pellets sintered under inert conditions, the measured specific surface areas and oxidation behavior are summarized in Table II, and the TGA oxidation behavior is illustrated by Figure 6. Optical micrographs of oxidized pellets are shown in Figure 7. Table II shows that sintering had a very large effect on the specific surface area, decreasing this by more than one order of

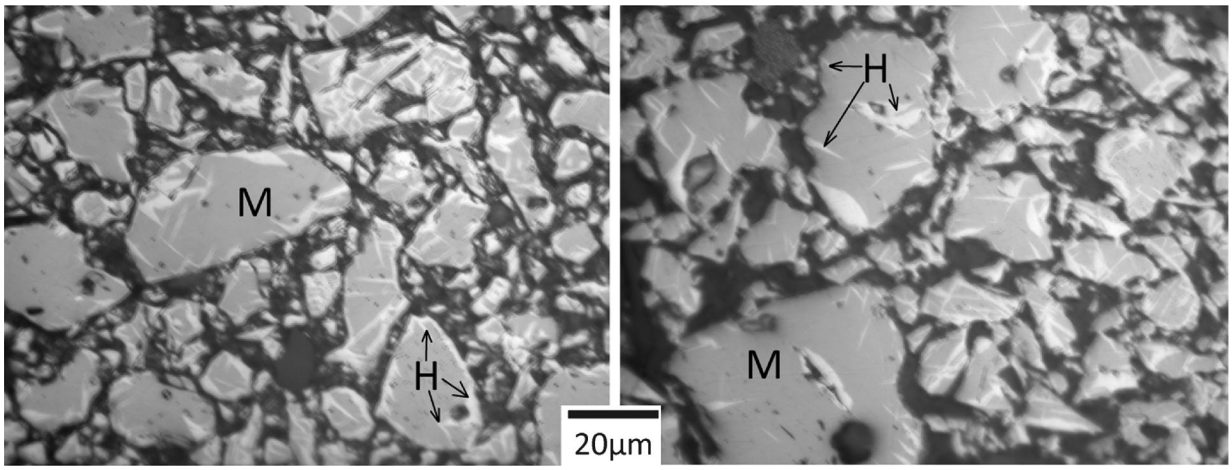

Fig. 7—Optical micrographs of pellets oxidized at 873 K (600 °C) for 30 min; pellets oxidized without any prior sintering (left; 59 pct oxidized), and after sintering at 1373 K (1100 °C) in argon for 30 min (right; 48 pct oxidized). Black areas are resin; dark areas (labeled "M") are unoxidized magnetite, and bright regions (labeled "H") are hematite.

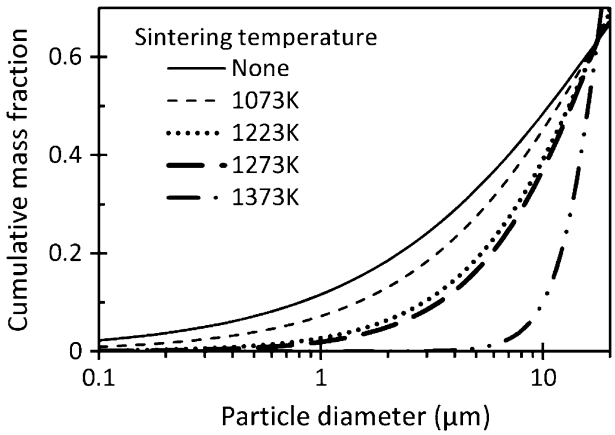

Fig. 8—Fitted Rosin-Rammler size distributions of magnetite particles in pellets sintered in argon at different temperatures for 30 min. Size distributions fitted to the measured specific surface area and degree of oxidation after 30 min at 873 K (600 °C).

magnitude (when comparing the pellet sintered at 1373 K [1100 °C] with the unsintered pellet). Based on the observed oxidation kinetics and specific area, it is estimated (as discussed below) that sintering at 1373 K (1100 °C) would mainly eliminate particles less than approximately 5 μm in diameter. This calculation agrees qualitatively with the optical micrographs in Figure 7, which show only minor changes in the particles visible at the resolution of optical microscopy.

The degree of oxidation after 30 minutes at 873 K (600 °C) was lower for sintered pellets (Figure 6 and Table II), but the effect of sintering on oxidation was not nearly as strong as was the effect on the specific surface area. This is as expected from the difference in the particle size range which most strongly affects the specific surface area, compared with the size range which affects oxidation. Particles smaller than 1 μm contribute most to the specific surface area. However, since all particles smaller than approximately 5 μm oxidized fully under these conditions, sintering would only affect the degree of oxidation strongly if most particles were to increase to larger than this size. The optical micrograph indicates that, even after sintering at 1373 K (1000 °C), some particles remain smaller than 5 μm.

Figure 6 shows that, during the initial period of approximately 5 minutes, when the oxidation rate is partially limited by gaseous mass transfer, oxidation of a pellet sintered at 1273 K (1000 °C) was slightly faster than that of an unsintered pellet. This probably reflects the increase in average pore size within the pellet after sintering; increased pore size would increase the Knudsen diffusivity.

The relationships illustrated in Figure 5 allow the parameters of the size distribution to be estimated from the degree of oxidation and specific surface area. In fitting these values, it was found that d^* showed no clear dependence on sintering; all the results could be fitted well with the same value of d^*, and hence only n was fitted separately for each sintering condition.

The estimated parameters are given in Table II, and graphs of the resulting estimated size distributions are shown in Figure 8. In Figure 8, the size distributions are truncated at a maximum size of 20 μm: Because both the degree of oxidation and the specific surface area are insensitive to particles larger than approximately 10 μm, the size distributions cannot be expected to accurate at the larger particle sizes. Both Table II and Figure 8 illustrate that n is estimated to become larger upon sintering, reflecting a narrower size distribution. This is as expected because small particles are eliminated by sintering.

An important practical effect of the size distribution is its effect on the plateau oxidation level ("f" in Figure 5). As shown in the companion paper, a *lower* plateau level would beneficially promote more uniform oxidation of pellets under conditions where gaseous diffusion of oxygen into the pellets is partially rate-limiting.[5] As Figure 5 illustrates, a lower plateau level can be obtained by increasing the average particle size (d^*) and by ensuring a narrower size distribution (larger n). While fine grinding of taconite ore is

essential to obtain liberation of magnetite particles from gangue, this work suggests that changes in the ore grind can have large effects on concentrate oxidation. To obtain a lower plateau level, a greater portion of large particles (greater than 5 μm) is required; given the quadratic dependence of oxidation time on particle size (Eq. [1]), changes in the detailed distribution of particles smaller than 5 μm would have little effect on overall oxidation behavior—all sub-5-μm particles would oxidize readily. Rather, obtaining a lower plateau level requires maximizing the proportion of particles larger than 5 μm.

Based on these observations, it is suggested that pellet plants can improve the uniformity of pellet oxidation by maximizing the proportion of particles larger than 5 μm in the magnetite concentrate.

IV. CONCLUSIONS

The observed effect of prior sintering of magnetite pellets on subsequent oxidation behavior at 873 K (600 °C) is consistent with the suggestion that the generally observed plateau-like oxidation behavior pellets results from the wide size distribution of the magnetite particles that constitute the pellets. The pellet oxidation behavior can be predicted from measured parabolic rate constants and estimated size distributions. Such quantitative relationships would be useful in predicting pellet oxidation under mixed-control conditions, where the oxygen content of the gas atmosphere affects oxidation, and unreacted magnetite cores may persist.

ACKNOWLEDGMENTS

Support of this project by the members of the Center for Iron and Steelmaking Research is gratefully acknowledged.

REFERENCES

1. H.J. Cho and P.C. Pistorius: *AISTech 2011 Proceedings Volume I*, Association for Iron and Steel Technology, Warrendale, PA, 2011, pp. 507-14.
2. S.R.B. Cooke and T.E. Ban: *Mining Eng*., 1952, vol. 6, pp. 1052–58.
3. H. Kokal: MSc Thesis, University of Minnesota, Minneapolis, 1970.
4. J.D. Zetterstrom: *Bureau of Mines Report of Investigations 4728*, United States Department of the Interior, Washington, DC, 1950.
5. M. Tang, H.J. Cho, and P.C. Pistorius: *Metall. Mater. Trans. B*, in press.
6. S.P.E. Forsmo, S.-E. Forsmo, P.-O. Samskog, and B.M.T. Björkman: *Powder Technol*., 2008, vol. 183, pp. 247–59.
7. B.E. Monsen, S.E. Olsen, and L. Kolbeinsen: *Scand. J. Metall*., 1994, vol. 23, pp. 74–80.
8. V. Niiniskorpi: Academic dissertation, Åbo Akademi, Åbo, Laboratory of Inorganic Chemistry, 2004, pp 54–55.
9. D. Papanastassiou and G. Bitsianes: *Metall. Trans*., 1973, vol. 4, pp. 487–96.
10. K. Meyer, H. Rausch, and M. Ottow: *Stahl und Eisen*, 1967, vol. 87, pp. 654–60.
11. P. Rosin and E. Rammler: *J. Inst. Fuel*, 1933, vol. 7, pp. 29–36.
12. K.M. Djamarani and I.M. Clark: *Powder Technol*., 1997, vol. 93, pp. 101–8.
13. H.P. Klug and L.E. Alexander: *X-Ray Diffraction Procedures for Polycrystalline and Amorphous Materials*, 2nd ed., John Wiley & Sons, New York, NY, 1974, pp. 493–4.
14. H.J. Cho and P.C. Pistorius: *AISTech 2012 Proceedings*, Association for Iron and Steel Technology, Warrendale, PA, 2012, pp. 503-11.
15. J. Païdassi: *Acta Metall*., 1958, vol. 6, pp. 219–21.
16. G.J. Yurek, J.P. Hirth, and R.A. Rapp: *Oxid. Met*., 1974, vol. 8, pp. 265–81.